Determination of the Upper Limit to the Electric Dipole Moment of the Electron at High Momentum Transfer*

R. E. RAND
High-Energy Physics Laboratory, Stanford University, Stanford, California
(Received 24 May 1965)

A new limit on the electron's electric dipole moment at high momentum transfer has been determined by scattering 100-MeV electrons at 180° from C^{12} nuclei. A full discussion of the theory involved and the experimental corrections due to multiple scattering, etc. is given. Assuming that the electron possesses no spurious magnetic moment, apart from the well-established Dirac and anomalous moments, its electric dipole moment is $\lesssim 2.3\times10^{-16}$ e cm at a momentum transfer of 1.0 fermi^{-1}. (A more detailed interpretation of the experiment is discussed in the conclusion.) The result is consistent with time-reversal invariance in quantum electrodynamics.

I. INTRODUCTION

In order to investigate a particular aspect of the ultimate validity of quantum electrodynamics (QED), the invariance under time reversal,[1] various attempts have been made to observe an electric dipole moment (EDM) in the electron and muon. Limits on the static EDM's of other elementary particles have been set by Smith, Purcell, and Ramsey[2] on the neutron ($\lesssim 3\times10^{-20}$ e cm) and by Sternheimer[3] on the proton ($\lesssim 1\times10^{-13}$ e cm). Berley and Gidal[4] have used a magnetic-deflection method in showing that the EDM of the muon is $\lesssim 2\times10^{-16}$ e cm.

Early estimates of the static EDM of the electron were made by Salpeter,[5] who considered the conservation of parity in atomic transitions and by Feinberg,[6] who analyzed the Lamb-shift experiments and concluded that the EDM is $\lesssim 10^{-13}$ e cm. Nelson *et al.*[7] have analyzed the electron-precession experiment of Schupp, Pidd, and Crane[8] and shown that the upper limit was $\lesssim 3\times10^{-15}$ e cm.

A recent determination of the limits of the static EDM of the electron has been reported by Sandars and Lipworth[9] who deduce their result from the absence of an EDM in the cesium atom using an atomic-beam technique. They obtain an upper limit of $\lesssim 2\times10^{-21}$ e cm.

All the above determinations have been made at very low energies and it is pertinent to inquire whether an EDM might be observed in high-momentum-transfer experiments, in which very short distances may be probed and a breakdown of QED would seem more feasible. This possibility has been pursued by investigating electron scattering from spin-zero nuclei as suggested by Margolis, Rosendorf, and Sirlin[10] and Avakov and Ter-Martirosyan.[11] The results of such experiments are indicated in Table I.[12,13] These results have been calculated assuming that the electron is a Dirac particle, whereas (as Margolis, Rosendorf, and Sirlin have suggested) positive results might be accounted for by an anomaly in the theoretical magnetic dipole moment (MDM), i.e., the electron might have a spurious MDM distinct from the established Dirac and anomalous moments. This point will be discussed more fully in the conclusion.

II. THEORY OF THE METHOD

Margolis, Rosendorf, and Sirlin have calculated the scattering of an electron, having an EDM, by a spin-zero nucleus by assuming that the coupling of the electron to the electromagnetic field is modified in the form:

$$e\gamma^\mu A_\mu \rightarrow e\gamma^\mu A_\mu + (ie\lambda/2m_0)\sigma^{\mu\nu}\gamma_5 F_{\mu\nu}\,,$$

where λ is the EDM in units $(e\hbar/m_0c)$. A further term

TABLE I. Upper limits of the electron's electric dipole moment (λ in units $e\hbar/m_0c$) obtained at high-momentum transfers by electron scattering.

Momentum transfer (F^{-1})	Scattering nucleus and angle	λ	Author
1.5–2.5	He^4 60°, 135°	$\lesssim 2\times10^{-4}$	Burleson and Kendall[a]
0.44	He^4 180°	$\lesssim 5\times10^{-5}$	Goldemberg and Torizuka[b]
1.00	C^{12} 180°	$\lesssim 6\times10^{-6}$	Present experiment

[a] See Ref. 12. [b] See Ref. 13.

* Research supported in part by the U. S. Office of Naval Research, Contract No. Nonr 225(67), and the U. S. Air Force Office of Scientific Research.

[1] L. Landau, Nucl. Phys. **3**, 127 (1957).
[2] J. H. Smith, E. M. Purcell, and N. F. Ramsey, Phys. Rev. **108**, 120 (1957).
[3] R. M. Sternheimer, Phys. Rev. **113**, 828 (1959).
[4] D. Berley and G. Gidal, Phys. Rev. **118**, 1086 (1960).
[5] E. E. Salpeter, Phys. Rev. **112**, 1642 (1958).
[6] G. Feinberg, Phys. Rev. **112**, 1637 (1958).
[7] D. F. Nelson, A. A. Schupp, R. W. Pidd, and H. R. Crane, Phys. Rev. Letters **2**, 492 (1959).
[8] A. A. Schupp, R. W. Pidd, and H. R. Crane, Phys. Rev. **121**, 1 (1961).
[9] P. G. H. Sandars and E. Lipworth, Phys. Rev. Letters **13**, 718 (1965).
[10] B. Margolis, S. Rosendorf, and A. Sirlin, Phys. Rev. **114**, 1530 (1959).
[11] G. V. Avakov and K. A. Ter-Martirosyan, Nucl. Phys. **13**, 685 (1959).
[12] G. R. Burleson and H. W. Kendall, Nucl. Phys. **19**, 68 (1960).
[13] J. Goldemberg and Y. Torizuka, Phys. Rev. **129**, 2580 (1963). J. Goldemberg (private communication). Uncertainties in the solid angle used in this experiment have increased the dipole limit from the published value.

may be added to this coupling to account for a spurious MDM in the form

$$(eK/2m_0)\sigma^{\mu\nu}F_{\mu\nu},$$

where K is the MDM in units $(e\hbar/m_0c)$. (This assumption distinguishes the spurious MDM from the anomalous MDM, whose contribution to the cross section is through multiple-photon exchange terms.)

Using these couplings, the cross section has been recalculated in first Born approximation to account for the nuclear recoil giving the result

$$\frac{d\sigma}{d\Omega}(\theta)=\frac{RF^2(q_\theta^2)}{\zeta(\theta)\sin^4(\theta/2)}\left\{\cos^2(\theta/2)+\frac{1}{\gamma^2}\sin^2(\theta/2)\right.$$
$$\left.\times\left[\frac{E_0}{Mc^2}+\left(1+\frac{2K\beta^2\gamma^2}{\zeta(\theta)}\right)^2+\frac{4\lambda^2\beta^2\gamma^4}{\zeta(\theta)}\right]\right\}, \quad (1)$$

where $R=Z^2e^4/4E_0^2$, $F(q_\theta^2)$ is the nuclear (charge) form factor,[14] $\hbar q$ is the momentum transfer,

$$\zeta(\theta)=1+(2E_0/Mc^2)\sin^2(\theta/2),$$

M is the nuclear mass, and $\gamma=E_0/m_0c^2$. This formula agrees with that of Margolis, Rosendorf, and Sirlin in the limit of an infinitely heavy nucleus. It should be noted that the K-dependent term given by Avakov and Ter-Martirosyan and used by Burleson and Kendall[12] and by Goldemberg and Torizuka[13] is incorrect for an electron of finite mass. In the above expression approximations are made only in the recoil corrections.

To investigate the possibility of the spurious MDM or EDM, (1) indicates that it is advantageous to measure the cross section at a scattering angle of 180° as first demonstrated by Goldemberg and Torizuka. If one writes $\xi=\pi-\theta$ (where ξ is <0.1, say) and ignores the recoil correction in the square bracket, (1) becomes:

$$\frac{d\sigma}{d\Omega}(\pi-\xi)=[RF^2(q_\pi^2)/\zeta(\pi)]\times\{(\xi^2/4)+(1/\gamma^2)I\}, \quad (2)$$

where

$$I=[(1+2K\gamma^2)^2+4\lambda^2\gamma^4].$$

[$\hbar^2q^2=4pp_0\sin^2(\theta/2)$ and $\zeta(\theta)$ vary only very slowly near $\theta=\pi$.[15]]

[14] A possible electron form factor may be included in $F(q_\theta^2)$ without modifying the form of the cross section (1).

[15] The cross section (2) is not strictly complete to order ξ^2. Allowing for the variation of momentum transfer with angle [i.e., $\hbar^2q^2=4pp_0(1-\xi^2/4)$], and assuming that the dipole moments are q-dependent, the curly bracket in (2) should be replaced by

$$\{(\xi^2/4)(1+\epsilon)+(1/\gamma^2)I(q_\pi^2)\},$$

where

$$\epsilon=\frac{I(q_\pi^2)}{\gamma^2}-4\left(\frac{m_0c}{\hbar}\right)^2\left(\frac{I(q_\pi^2)}{F^2(q_\pi^2)}\frac{dF^2(q^2)}{dq^2}\bigg|_\pi+\frac{dI(q^2)}{dq^2}\bigg|_\pi\right).$$

The question arises whether this extra term affects the logic of the arguments of Sec. VI. Assuming that the hypothetical dipole moments are significant and that their form factors are well behaved and Gaussian-like, one obtains

$$dI(q^2)/dq^2\simeq\tfrac{1}{3}a^2I(q^2),$$

where a is the rms radius of the dipole distributions. Any reasonable distribution would yield a derivative of similar order of magnitude. If it is further assumed that $a\lesssim10^{-13}$ cm and if the measured C^{12} form factors are used, one obtains $\epsilon\sim10^{-4}I(q_\pi^2)$. Thus the experimental result given in Sec. V should strictly be written

$$-0.2<I'<1.2,$$

where

$$I'=I(q_\pi^2)[1+10^{-4}I(q_\pi^2)]^{-1}.$$

Hence

$$|1/I'|=|1/I(q_\pi^2)+10^{-4}|>0.8,$$

and it is clear that the extra term may be neglected.

Measurement of the variation of this cross section with angle near 180° enables one to determine independently the nuclear form factor and I, allowing limits to be placed on K and λ.

McKinley and Feshbach[16] have shown that the second Born approximation to normal Mott scattering is of the form

$$RZ\pi\alpha\beta[\sin(\theta/2)-\sin^2(\theta/2)]/\sin^4(\theta)/2,$$

which becomes $\frac{1}{8}RZ\pi\alpha\beta\xi^2$ near 180° and does not contribute to the experimental value of I.

Goldberg[17] has examined two-photon exchange scattering in which the nucleus can be in an excited virtual state and concludes that any correction applicable to this type of experiment is small and of the same form as the Coulomb correction, provided $\hbar q/M_Nc\ll1$, (where M_N is the nucleon mass) so that again there is no contribution to I.

III. EXPERIMENTAL CONSIDERATIONS

In a practical experiment, the probability of an electron scattering at 180° from a spin-zero nucleus is not exactly zero for the following reasons:

(a) finite electron rest mass (Sec. 2);
(b) multiple scattering in the target;
(c) finite angular and spatial spread of the incident beam;
(d) finite solid angle.

The effects of (b), (c), and (d) were by no means negligible and were calculated as follows:

Electrons which enter the target and scatter at angles near 180° may traverse various thicknesses of target material up to (and beyond) twice the target thickness, so that a large energy spread in the scattered electron spectrum is to be expected. It is convenient to classify scattered electrons according to their total path length ($2t_p$) in the target. The expected distribution of scattered electrons may then be calculated as a function of t_p which corresponds very closely to the ionization energy loss in the target assuming that straggling is negligible and that the electron is a minimum ionizing particle. The effect of straggling and of energy spread of the incident beam may then be accounted for by

[16] W. A. McKinley, Jr. and H. Feshbach, Phys. Rev. **74**, 1759 (1948).

[17] A. Goldberg, Nuovo Cimento **20**, 1191 (1961).

suitably folding the appropriate distributions into the t_p distribution so that the shape of the scattered momentum spectrum may be obtained. However, this folding process is not essential as the total correction due to (b) in the elastic peak at 180° is given with sufficient accuracy by the t_p distribution. Radiation losses modify the momentum distribution obtained from the t_p distribution and must be allowed for in the data analysis.

The effect of (b) may be calculated for an electron with total path length in the target $2t_p$, by considering the scattering scheme illustrated in Fig. 1.

The probability of an electron arriving at the plane $t=t_p$ in the target, moving into the solid angle $\sin\theta d\theta d\Phi$ at (θ,Φ), where θ is measured with respect to the incident beam direction, may be written

$$\int_0^{t_p} P_{t_p}(t_1,\theta)dt_1 \sin\theta d\theta d\Phi .$$

The probability of further scattering at an angle $(\pi-\theta')$ into the element of solid angle $d\Omega$ in such a way that the total electron path in the target is between $2t_p$ and $2(t_p+dt_p)$ is

$$\sim\frac{N\rho}{A}\frac{2dt_p}{1+\cos\theta}\frac{d\sigma}{d\Omega}(\pi-\theta')d\Omega .$$

Thus the total probability of an electron multiply-scattering into a given solid angle $d\Omega$ is

$$T\simeq\frac{N\rho dt_p d\Omega}{A}\int_0^{\pi}\int_0^{2\pi}\int_0^{t_p} P_{t_p}(t_1,\theta)dt_1 \times\frac{2}{1+\cos\theta}\frac{d\sigma}{d\Omega}(\pi-\theta')\sin\theta d\theta d\Phi .$$

If the direction of $d\Omega$ with respect to the incident beam is $(\pi-\xi)$, then θ' is composed of the vector addition of angles θ and ξ. Φ may then be defined as the angle between the planes containing θ and ξ and it can be shown that

$$\int_0^{2\pi}\frac{d\sigma}{d\Omega}(\pi-\theta')d\Phi=2\pi\frac{d\sigma}{d\Omega}(\pi-\theta)[1+E(\theta)\xi^2+O(\xi^4)] .$$

The integral T may now be evaluated by first considering very small angles θ up to a limit θ_0. The distribution θ then follows the Molière[18] small-angle multiple-scattering theory so that

$$\int_0^{t_p} P_{t_p}(t_1,\theta)dt_1 \rightarrow f_{t_p}(\theta)/2\pi ,$$

where $f_{t_p}(\theta)$ is Molière's distribution. Also for small angles, $E(\theta)\rightarrow\theta^{-2}$. Thus, using (2), one obtains a

[18] G. Molière, Z. Naturforsch. **3a**, 78 (1948).

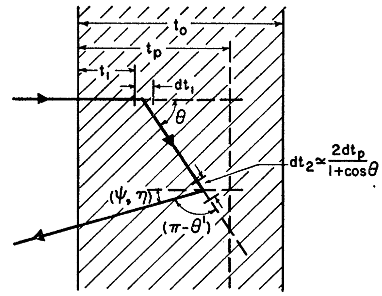

FIG. 1. Generalized 180° scattering of electrons from a thick target. $(\pi-\psi)$ and $(\pi-\eta)$ are horizontal and vertical projections (in the laboratory) of the scattering angle defined by the detector. The diagram is drawn in the plane of the first scatter.

contribution to T:

$$\frac{N\rho dt_p d\Omega}{A}\int_0^{\theta_0} f_{t_p}(\theta)\theta d\theta\frac{RF^2(q_\pi^2)}{\zeta(\pi)}\left\{\frac{\theta^2+\xi^2}{4}+\frac{1}{\gamma^2}\right\}$$
$$\simeq\frac{N\rho dt_p d\Omega}{A}\frac{RF^2(q_\pi^2)}{4\zeta(\pi)}\left\{\langle\theta^2\rangle_{\mathrm{MS}}+\xi^2+\frac{4}{\gamma^2}\right\} , \quad (3)$$

where $\langle\theta^2\rangle_{\mathrm{MS}}$ is the mean-square multiple-scattering angle in the range $0\le\theta\le\theta_0$. Integration in the range $\pi-\theta_0\le\theta\le\pi$, yields a further contribution $\langle\theta^2\rangle_{\mathrm{MS}}$ to the curly bracket in (3).

The evaluation of T for intermediate angles involves the use of Molière's large-angle modification to the Mott scattering cross section, i.e.,

$$P_{t_p}(t_1,\theta)=(N\rho/A)[RF^2(q_\theta^2)/\zeta(\theta)] \times[\cos^2(\theta/2)/\sin^4(\theta/2)][1/(1-K/\theta^2)] ,$$

where K is essentially constant for a given t_p. If θ_0 is chosen so that $\xi^2\ll\theta_0^2\ll1$, then $E(\theta)\xi^2\ll1$ for the intermediate angles and the remaining part of T is given by

$$16\pi(N\rho/A)^2dt_p d\Omega[R^2F^2(q_\pi^2)/\zeta(\pi)]\times C ,$$

where

$$C\simeq\int_0^{t_p}\int_{\theta_0}^{\theta_{\max}(t_1)}\frac{(1+K/\theta^2+K^2/\theta^4)}{\sin\theta(1+\cos\theta)}d\theta dt_1 .$$

For $0\le t_p\le t_0$ one obtains

$$C\simeq t_p(\ln(2/\theta_0)+\tfrac{1}{2}+K/2\theta_0^2+K^2/4\theta_0^4) .$$

(Terms of order $t_p\theta_0^2$ are ignored). Thus the effective experimental scattering cross section for t_p may be written

$$\langle d\sigma/d\Omega\rangle_{t_p}=[RF^2(q^2)/4\zeta(\pi)] \times\{\xi^2+2\langle\theta^2\rangle_{\mathrm{MS}}+\langle\theta^2\rangle_{\mathrm{DS}}+(4/\gamma^2)I\} , \quad (4)$$

where

$$\langle\theta^2\rangle_{\mathrm{DS}}=64\pi R(N\rho/A)\times C .$$

The finite angular spread of the beam may now be taken into account by adding a further term $\langle\theta^2\rangle_{\mathrm{B}}$ to the curly bracket in (4). If the angular spread is caused

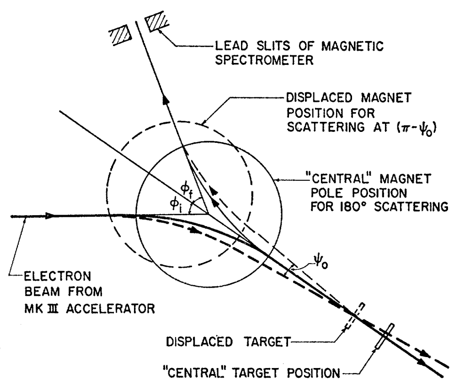

FIG. 2. Principle of the 180° scattering apparatus.

by the beam passing through a thin foil before reaching the target, as in the present apparatus, $\langle\theta^2\rangle_B$ may be conveniently calculated from the Gaussian approximation of Hanson *et al.*[19] to the small-angle Molière theory, as large angles are not important in this case. Spatial spread of the beam may be included in $\langle\theta^2\rangle_B$ but is negligible in practice.

Finally (4) must be integrated over the experimental solid angle, which may be represented by limits of the form $\psi_0\pm\Delta\psi$ and $\pm\Delta\eta$ in the present geometry, where ψ and η are, respectively, the projections of ξ on horizontal and vertical planes containing the incident beam line. This yields an effective total cross section (in the path-length range $2dt_p$):

$$\Delta\sigma=[RF^2(q_\pi^2)/4\zeta(\pi)]\{\psi_0^2+\tfrac{1}{3}(\Delta\psi^2+\Delta\eta^2)+2\langle\theta^2\rangle_{\mathrm{MS}}+\langle\theta^2\rangle_{\mathrm{DS}}+\langle\theta^2\rangle_{\mathrm{B}}+(4/\gamma^2)I\}4\Delta\psi\Delta\eta. \quad (5)$$

In the present experiment, the object of which was to measure I, all terms in (5) were significant.

IV. APPARATUS

The experiment consisted of scattering 100-MeV electrons at $\sim$180° from C^{12} nuclei. Backward scattering was achieved with an apparatus similar in principle to that used by Goldemberg and Torizuka[13] and first described by Peterson and Barber.[20] This principle is illustrated in Fig. 2 where scattered electron trajectories for an infinitely heavy nucleus are shown (i.e., $\Phi_i=\Phi_f$). For finite nuclei $\Phi_f>\Phi_i$, but the cylindrical symmetry of the magnetic field enables the effective solid angles and scattering angles to be easily determined.

Figure 3 shows the practical details of the apparatus. With the magnet in its "central" position, electrons from the Stanford Mark III linear accelerator enter the uniform magnetic field radially and after being deflected about 35°, pass out of the field region and through the target. Those electrons scattered at $\sim$180° pass through the field a second time and are analyzed by a vertical 180°, $n=\frac{1}{2}$ magnetic spectrometer (of mean orbit radius 72 in.), where they are detected by a 10-channel scintillator ladder, each channel corresponding to a different momentum.

The scattering chamber is rigidly fixed inside the deflection magnet and isolated from the beam tube vacuum system by 0.001-in. aluminum windows. The two magnets and the chamber may be moved on tracks along the line of the beam after its first deflection. This enables one to calibrate the beam monitor, an aluminum secondary-emission monitor, by removing the deflection

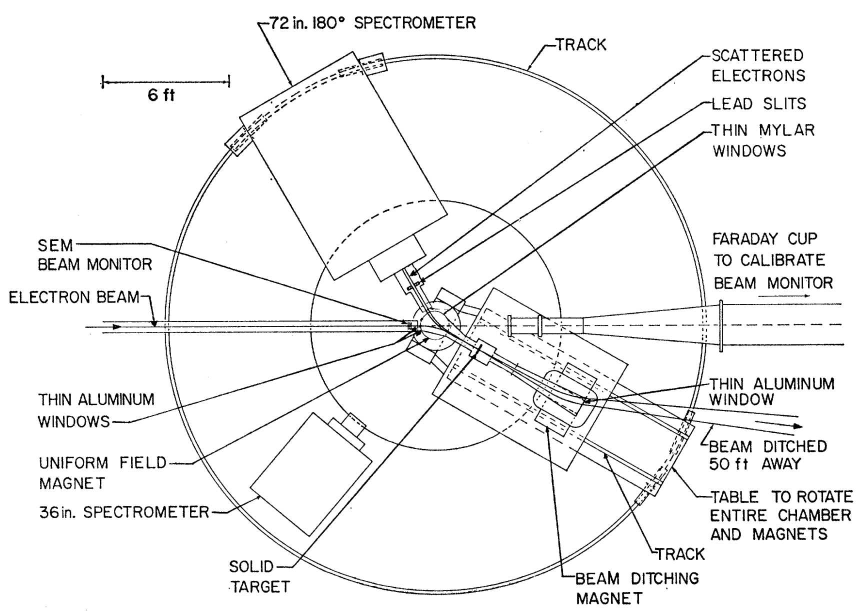

FIG. 3. Experimental arrangement for 180° scattering.

[19] A. O. Hanson, L. H. Lanzl, E. M. Lyman, and M. B. Scott, Phys. Rev. 84, 634 (1951).
[20] G. Peterson and W. C. Barber, Phys. Rev. 128, 812 (1962).

magnet and collecting the beam in the Faraday cup. With the deflection magnet removed it is also possible to raise a fluorescent screen into the beam line. This is located exactly at the center of the deflection magnet when the latter is in its "central" position and enables one to ensure that the beam enters the magnet radially in that position.

It has already been indicated that in order to subtract the finite charge scattering at 180°, it is necessary to vary the scattering angle a few degrees either side of the backward direction. This provides a value for $F^2(q_\pi^2)$.

The most obvious way to do this is to vary the angular position of the spectrometer. However, if this instrument is to be used at its maximum solid angle, the mean electron trajectory must enter the slits along the optic axis. Any small deviation from this condition severely restricts the available solid angle and only scattering angles very close to 180° (say $\pm 1°$) can be obtained. Goldemberg and Torizuka varied the scattering angle by varying the magnetic field. This method also suffers from the same disadvantage however.

Figure 2 indicates how the scattering angle was varied in this experiment. A displacement of the magnet and target along the line of the beam at the target, together with a slight change in the magnetic field, enabled the scattering angle to be varied to 174° on either side with only a small change in the solid angle. The variations of the scattering angle and solid angle with this displacement, and with scattered electron momentum were calculated to second order and verified by a floating-wire method.

The experiment was performed at as high an energy as possible, to set low limits on the dipole moments, but was restricted to 100 MeV by the rapid decrease of the C^{12} form factor with momentum transfer. The most significant results have been obtained with carbon targets of 0.607 and 0.303 g/cm^2.

V. ANALYSIS OF THE DATA

Two or three settings of the spectrometer and up to six scattering angles (deflection-magnet positions) were used for each target.

It has been noted that the scattering angle and solid angle are functions of both momentum and magnet position. Consequently the counts obtained in each momentum channel were corrected to a standard solid angle (after background subtraction, etc.) and a least-squares fit of a parabola, of the form (5) was made to the various angular settings for each momentum channel. Some of these parabolas in a particular experiment are shown in Fig. 4.

The counts due to the ψ_0^2 term in (5), which would have been obtained at 179°, were calculated for each channel from the parabolas resulting in an "elastic peak" as shown in Fig. 5(a).

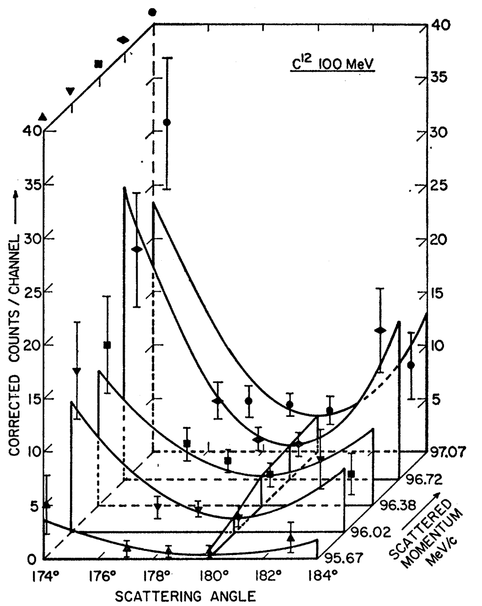

FIG. 4. Some of the data from one particular experiment illustrating the variation with angle of the elastic electron-C^{12} scattering cross section near 180°. Note that the experimental points for one particular deflection magnet setting do not lie at a constant scattering angle.

The counts which would have been obtained at exactly 180° were then corrected for the finite solid angle, finite beam spread, electron rest mass (assuming $I=1$) and the multiple scattering effects, assuming that energy loss was strictly proportional to the path length in the target. This resulted in distributions of the form shown in Fig. 5(b). The small peak at 96.3 MeV is due to ignoring the straggling and beam energy spread, but this does not effect the sum of the counts at 180°.

The counts at 179° were corrected for the overlapping channels and then for radiation effects. The spectrum which would have been obtained if no radiation losses had occurred is shown by the dashed line in Fig. 5(a). From this a value of the C^{12} form factor could be ob-

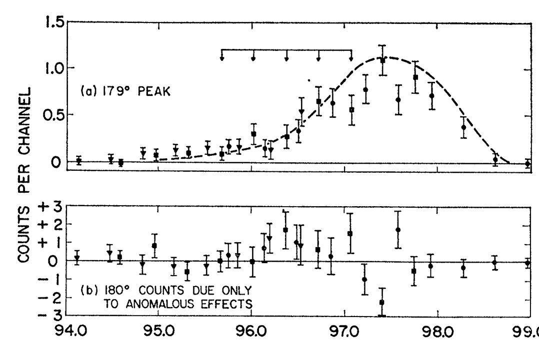

FIG. 5. Typical "elastic peaks" for electron-C^{12} scattering at 179° and 180° (see text). The indicated channels correspond to the data shown in Fig. 4. The dashed line is the charge peak at 179° corrected for radiation effects.

TABLE II. Experimental results. $F^2(q^2)$ is the measured charge form factor and I is the coefficient of $1/\gamma^2$ in the theoretical expression (2). The goodness of fit to the expected angular distribution (5) is also given.

Target (g/cm^2)	$F^2(q^2)$	I	Fit to expression (5) χ^2	Degrees of freedom
0.607	0.143±0.011	1.0±1.2	101.4	120
0.303	0.132±0.010	1.0±1.3	96.6	80
0.303	0.127±0.010	−0.5±1.2	34.6	40

tained to check the efficiency of the apparatus and to calculate the experimental value for I.

Before I was calculated from the effective counts at 180°, these were adjusted to allow for the radiative effects ignored in the multiple-scattering correction. Figure 4 demonstrates how the momentum spectrum at 180° is much flatter than that at smaller angles due to the multiple-scattering effects.

Finally, a small correction was applied for magnetic scattering from the 1.1% C^{13} in natural carbon.

Results of three runs are shown in Table II. No significant dependence on target thickness beyond the calculated multiple-scattering effects was apparent.

Each run exhibited a reasonable χ^2 fit to the expression (5) and gave a value of the C^{12} form factor consistent with the accepted value.[21] The weighted mean experimental result is

$$I=(1+2K\gamma^2)^2+4\lambda^2\gamma^4=0.5\pm0.7 \quad \text{at} \quad q^2=1.00\ \text{F}^{-2}.$$

VI. CONCLUSIONS

If the experimental value of I is to be interpreted in terms of spurious magnetic and electric dipole moments of the electron, certain assumptions must be made about these quantities.

Firstly, if λ and K are both assumed to be nonzero and to be dependent on the momentum transfer, no information from previous low-energy experiments can be invoked. Under these conditions, one obtains the following limits at the 68% confidence level:

$$|\lambda|\leq1.4\times10^{-5}, \quad -1.3\times10^{-5}\leq K\leq0.1\times10^{-5}.$$

If, however, one uses the low-energy experimental limit on K,[8,22] i.e., $K\lesssim4\times10^{-6}$, and assumes that it applies to this type of experiment, one obtains

$$|\lambda|\lesssim9\times10^{-6}, \quad \text{equivalent to } 3.5\times10^{-16}\ e\ \text{cm}.$$

Finally, if it is assumed that $K=0$ (as all previous authors in this field have done and as is assumed in Table I), one obtains

$$|\lambda|\lesssim6\times10^{-6}, \quad \text{equivalent to } 2.3\times10^{-16}\ e\ \text{cm}.$$

It is to be noted that even in a perfect experiment of the present type, assuming that λ and K are q-dependent, the ultimate limits obtainable are

$$-1/2\gamma^2\leq K\leq0 \quad \text{and} \quad |\lambda|\leq1/2\gamma^2.$$

In this case,

$$1/2\gamma^2=1.3\times10^{-5}.$$

Consequently it is planned to perform this experiment at higher energies using a liquid-He^4 target and an improved apparatus. This will be advantageous both from the above point of view and because the He^4 form factor does not decrease as rapidly as that of C^{12}.

ACKNOWLEDGMENTS

The author would like to thank Professor R. Hofstadter for his active interest and encouragement in this work, and Professor L. I. Schiff for useful discussions on the validity of this and other experiments. He is also indebted to Professor M. R. Yearian for helpful suggestions concerning the analysis of the experimental data and for reading the manuscript, and to Dr. T. A. Griffy for assistance in checking the necessary theory.

[21] H. L. Crannell, Ph.D. thesis, Stanford University, 1964 (unpublished).

[22] S. D. Drell, Ann. Phys. (N. Y.) 4, 75 (1958).